International Journal of Pharmaceutics xxx (2015) xxx–xxx

Contents lists available at ScienceDirect

International Journal of Pharmaceutics

journal homepage: www.elsevier.com/locate/ijpharm

Pharmaceutical nanotechnology

Solubilization of menthol by platycodin D in aqueous solution: An integrated study of classical experiments and dissipative particle dynamics simulation

Haiou Ding [a,1], Qianqian Yin [b,1], Guang Wan [b], Xingxing Dai [c], Xinyuan Shi [c,d,e,*], Yanjiang Qiao [c,d,e,*]

[a] Civil Aviation General Hospital, No. 1 of Chaowai Takai A, Beijing 100123, China
[b] School of Traditional Chinese Medicine, Capital Medical University, Beijing 100069, China
[c] Beijing University of Chinese Medicine, Beijing 100102, China
[d] Key Laboratory of TCM-Information Engineer of State Administration, Beijing 100102, China
[e] Beijing Key Laboratory for Basic and Development Research on Chinese Medicine, Beijing 100102, China

ARTICLE INFO

Article history:
Received 19 September 2014
Received in revised form 19 December 2014
Accepted 18 January 2015
Available online xxx

Chemical compounds studied in this article:
Menthol (PubChem CID: 16666)
Platycodin D (PubChem CID: 162859)

Keywords:
Biosurfactants
Platycodin D
Menthol
Solubilization
Dissipative particle dynamics

ABSTRACT

Menthol (M) and platycodin D (PD) are the main active ingredients in *Mentha haplocalyx* and *Platycodon grandiflorum* A. DC., respectively. They are commonly used in combination in traditional Chinese medicine. In this study, laboratory experiments and computer simulations were used to investigate the solubilization of M by PD, which was believed to be one of the main causes of the synergistic effect of *M. haplocalyx* and *P. grandiflorum* A. DC. Results showed that both the method by which M was added and the concentration of PD had significant effects on the solubilization efficiency of M, and these influences were closely associated with each other. Temperature, an important environmental condition, was also found to have a significant effect on the solubilization effect of PD. These findings not only clarify the molecular basis of the solubilization effect, including amount solubilized at the macroscale and the structures of the micelles, and the drug loading mechanisms and processing at the mesoscale. This work may provide some guidance for the further development of saponins and fundamental research in the drug delivery system.

1. Introduction

There is a growing interest in biosurfactants because of their excellent functional properties, wide availability, low cost, and biological and environmental safety (Rodrigues et al., 2006; Urum and Pekdemir, 2004). Saponin is one of the most commonly known plant-based surfactants and has been widely used in the pharmaceutical industry as a solubilizer and emulsifier and in other capacities (Itoh et al., 1986; Kulperger, 1996; Mukherjee et al., 2006; Soeder et al., 1996). They function well in improving the solubility of hydrophobic drugs, and many of them show significant pharmacological activity, which allows them to play a dual role in compound preparation (Walthelm et al., 2001; Sasaki et al., 1988).

Platycodon grandiflorum A. DC. (Campanulaceae) is a well-known traditional Chinese medicine used as an expectorant for pulmonary diseases and as a remedy for respiratory disorders (Sun et al., 2011). It is generally used in combination with *Mentha haplocalyx* to generate synergistic therapeutic effects. Their main active ingredients are platycodin and mint oil, respectively (Chengyuan et al., 2003; Haiping et al., 2012; Guo et al., 2007b). Menthol (M) has many types of pharmacological activity, including anti-inflammatory, analgesic, anti-fungal, and central nervous system excitation effects. It has been used for the treatment of coughing, headaches, itching, mycotic infections, and diaphoresis (Jiangsu, 1986). It has been reported that platycodin D (PD) can increase the solubility of M efficiently because it can form micelles in aqueous solutions during the preparation process. This is considered a possible mechanism of the synergistic therapeutic effect (Yanjun and Jinming, 2011). However, the solubilization mechanisms and the colloidal properties of the micelles, such as the

* Corresponding authors at: Beijing Key Laboratory or Basic and Development Research on Chinese Medicine, Beijing University of Chinese Medicine, No. 6, Wang Jing Zhong Huan Nan Lu, Beijing 100102, China. Tel.: +86 10 84738621; fax: +86 10 84738661.
E-mail addresses: xyshi@126.com (X. Shi), yjqiao@263.net (Y. Qiao).
[1] These authors contributed equally to this work.

http://dx.doi.org/10.1016/j.ijpharm.2015.01.033
0378-5173/

morphology and size, have not been investigated. The solubilization efficiency and the influence factors are not yet well understood.

In this study, experimental methods such as gas chromatography (GC), transmission electron microscopy (TEM), dynamic light scattering (DLS), and computer simulation methods such as dissipative particle dynamics (DPD), MesoDyn were used in this study to evaluate the solubilization effects in a thorough and comprehensive manner. GC is a widely used method of quantitative analysis of volatile constituents, so it was used here to measure menthol content in solutions before and after solubilization to determine the amount solubilized. Mature methods of observing micelle morphology, TEM and DLS, were used to determine the colloidal properties of PD micelles, including the morphology and size. However, factors affecting the mechanisms underlying solubilization, such as the exact internal structure of PD micelles, the loading position of M, and the dynamic solubilization process, were not observable using conventional laboratory methods. Computer simulation is an effective and intuitive technique based on Newton's equation of motion, and it is increasingly used in the study of intramolecular and intermolecular interactions. Modern advances in dynamic methodologies and the excellent performance of modern computers have facilitated investigations of physical processes and their interactions in watery environments in detail (Buxton and Clarke, 2007; Ding et al., 2013; Guo et al., 2007a; Ramos-Rodríguez et al., 2010). By changing molecular resolution, which is generally known as mesoscopic or coarse-grain (CG), we can obtain larger temporal and spatial scales during a simulation (Ingólfsson et al., 2013). Dissipative particle dynamics (DPD) and MesoDyn are effective mesoscopic simulation techniques. DPD, a particle-based method of mesoscale simulation, allows soft coarse-grained particles to interact through a simple-wise potential and to thermally equilibrate through hydrodynamics on a mesoscopic scale (Groot and Warren, 1997; Hoogerbrugge and Koelman, 1992). DPD not only can capture the hydrodynamic behavior of fluids and the underlying interactions of the species accurately, but also can directly present the movement of mesomolecules, which MesoDyn simulation cannot do. But MesoDyn is a method based on a dynamic variant of mean-field density functional theory. It has the advantage of allowing the investigation of the microphase separation of block copolymers. (Accelrys, 2010; Fraaije et al., 1997)

In this work, laboratory experiments and computer simulation were combined to investigate the solubilization properties of PD. DPD was used to evaluate the mechanism of solubilization and visualize the dynamic solubilization process, and MesoDyn was used to study the effect of temperature on the solubilization effect of PD. First, the self-assembly morphologies of PD were investigated at different concentrations, and the effects of the concentration of PD, the method by which M was added, and temperature on the efficiency of solubilization in aqueous solution were discussed. The results obtained from laboratory and simulation were not only closely consistent but complemented each other well. It might facilitate better understanding of the solubilization effects of saponins and could provide some guidance for the development and fundamental research of saponins for use as solubilizers in drug delivery systems.

2. Materials and methods

2.1. Materials

PD (111851-201204, purity ≥98%) and M (110728-200506, purity ≥98%) were purchased from the National Institutes for Food and Drug Control and used without further purification. All other chemicals and solvents were of reagent grade or better.

2.2. Sample preparation

In this section, primarily blank PD solutions, M-loaded PD solutions, and saturated aqueous solutions of M were prepared. The influence factors taken into consideration included concentration of PD, method of addition M, time for solubilization, and temperature.

2.2.1. Preparation of blank PD aggregate solutions

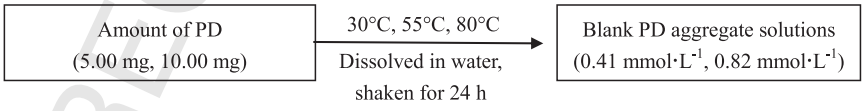

2.2.2. Preparation of M-loaded PD aggregate solutions

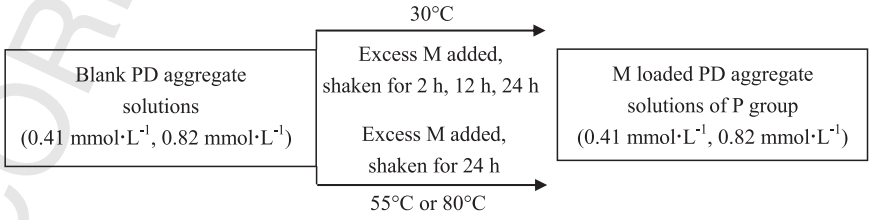

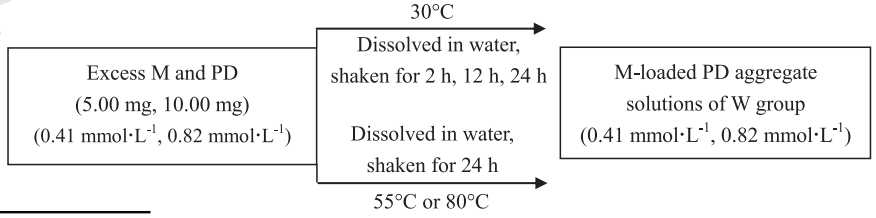

2.2.3. Preparation of saturated aqueous solutions of M

The saturated aqueous solution of M was used as reference solution for each group in Section 2.2.2 and prepared by dissolving excess M in water and then processing under the same conditions as in Section 2.2.2 (see Supplementary data for more information).

Please cite this article in press as: Ding, H., et al., Solubilization of menthol by platycodin D in aqueous solution: An integrated study of classical experiments and dissipative particle dynamics simulation. Int J Pharmaceut (2015), http://dx.doi.org/10.1016/j.ijpharm.2015.01.033

2.3. Transmission electron microscopy

The morphology of the micelles was observed using transmission electron microscopy (TEM) (TEM, JEOL JEM-1230 microscope) operated at an acceleration voltage of 80 kV.

2.4. Dynamic light scattering measurement

DLS studies were performed using a Zetasizer Nano-ZS instrument (Malvern Instruments, Malvern City, U.K.) at 30 °C at a scattering angle of 173°. The intensity-average diameter and particle dispersion index (PDI) of micelles were calculated and averaged 10 ten runs of 30 s each.

2.5. Gas chromatography (GC) analysis

All GC measurements were carried out using a headspace sampler (Agilent HP-7694E) and gas chromatography (Agilent HP-7890N) equipped with flame ionization detector (FID). Samples were analyzed in an HP-5 quartz capillary column (30 m × 0.32 mm × 0.25 μm, 5% phenyl-methyl silicone; Agilent Technologies, Santa Clara, U.S.). Headspace sampler operating conditions were set as follows: oven temp. = 60 °C; equilibration temp. = 80 °C; needle and sampling coil temp. = 90 °C; transfer temp. = 100 °C; vial equilibrium time = 10.0 min; vial pressurization time = 0.2 min; sample-loop fill time = 0.2 min; loop equilibration time = 0.05 min; loop fill time = 0.2 min. The temperature of both the flame ionization detector and the sample injection was set at 250 °C. High-purity nitrogen (99.99%) was used as the carrier gas.

3. Simulation details

3.1. Dissipative particle dynamics and MesoDyn

DPD was introduced by Hoogerbrugge and Koelman and modified by Groot and Madden (1998). It involves using Newton 's equation of motion to govern the time evolution of a many-body system through numerical integration. The position and velocity (r_i, v_i) of each particle at every iteration were inherited from an earlier point in time.

$$\frac{dr_i}{dt} = v_i, \qquad m_i \frac{dv_i}{dt} = f_i \tag{1}$$

For simplicity, the mass of all particles was set to 1 DPD unit, r_i, v_i, m_i, and f_i denote the position vector, velocity, mass, and total force acting on particle i, respectively. The sum f_i between each pair of beads contains three components: a harmonic conservative interaction force (F_{ij}^C), a dissipative force (F_{ij}^D), and a random force (F_{ij}^R). The expression is given as follows:

$$f_i = \sum_{j^1 i} (F_{ij}^C + F_{ij}^D + F_{ij}^R) \tag{2}$$

All forces are short-range with a fixed cut-off radius r_c, which is usually chosen as the reduced unit of length $r_c = 1$. All simulations were conducted in Materials Studios 5.5 (Accelrys, 2010)

To calculate the conservation force, Groot and Warren have made a link between the repulsive parameter (α_{ij}) and the Flory–Huggins parameters χ_{ij} (Groot and Warren, 1997). Solubility parameters δ, based on the chemical nature of species, can be obtained using the molecular dynamics (MD) simulation. And the repulsion parameters ε_{ij} used in MesoDyn were calculated according to formula (4).

$$\chi_{ij} = \frac{V}{RT}(\delta_i - \delta_j)^2 \tag{3}$$

$$\varepsilon_{ij} = \chi_{ij} RT \tag{4}$$

In this study, solubility parameters were calculated using the Discover module with the COMPASS force field. Both the repulsion parameters α_{ij} in DPD and ε_{ij} in MesoDyn are shown in Supplementary data (Tables S1, S2, and S3), respectively.

3.2. Model and simulation parameters

The components used in this simulation comprise of PD, M, and water. The coarse-grained models are shown in Fig. 1. The ring-like structure was considered as a unit, and the molecular structure of PD was mapped to three types of particles (A, B, and G) according to the polarity of the group they represent. Glycosyl units were represented by G type of particles, the ring-like groups in the aglycone linked with sugar chains are referred to as A type particles, and the other groups in the aglycone are referred as B type particles. The order of the polarity was G > A > B (Fig. 1a). Menthol and water are referred to as M and W, respectively (Fig. 1b and c).

Before starting systematic study of solubilization effect, we discussed the possible effect of system size on simulation outcomes in our pre-experiments, and the results are shown in Fig. S2 in Supplementary data. It can be seen that, when system size was $20 \times 20 \times 20\ r_c^3$ or larger, the morphology and size of aggregates showed no significant difference, but the computation cost resulting from increasing in system size became more expensive. Considering the simulation quality and computation efficiency, cell size in this paper was set to $20 \times 20 \times 20\ r_c^3$ (Fig. S2) and the integration time step was $0.05\ t_c$. The r_c and t_c are DPD

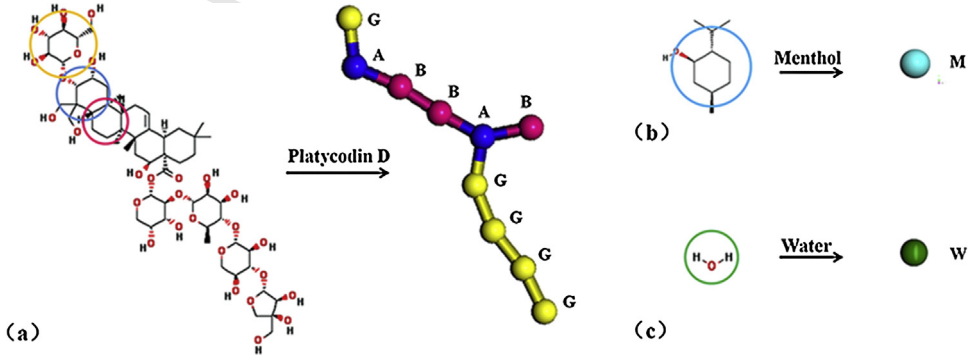

Fig. 1. Chemical structures and coarse-grained models. (a) PD; (b) M; (c) water.

Please cite this article in press as: Ding, H., et al., Solubilization of menthol by platycodin D in aqueous solution: An integrated study of classical experiments and dissipative particle dynamics simulation. Int J Pharmaceut (2015), http://dx.doi.org/10.1016/j.ijpharm.2015.01.033

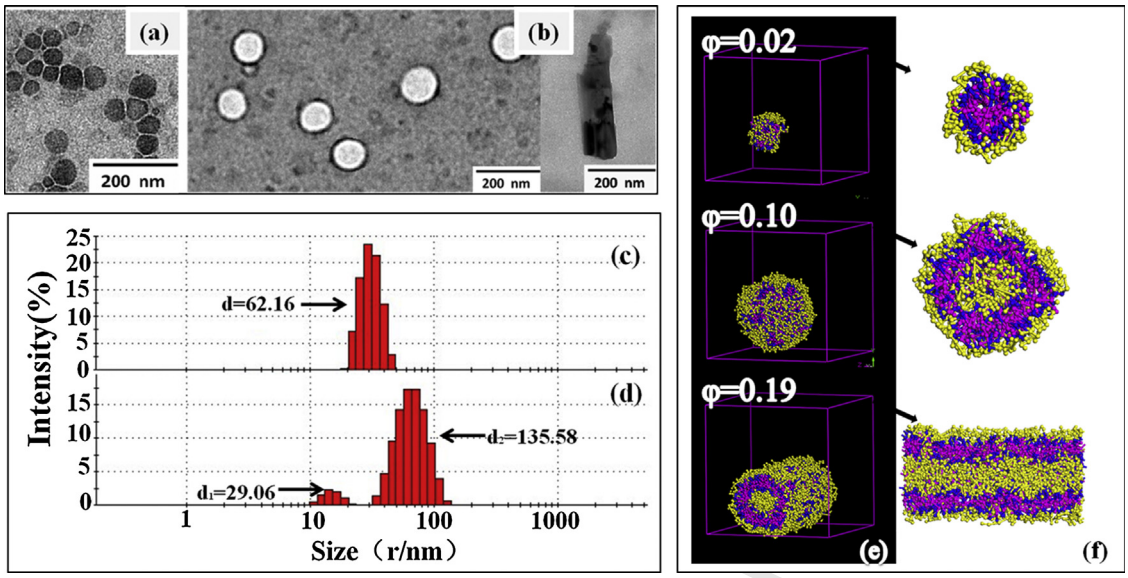

Fig. 2. Morphologies of blank PD aggregates. (a) TEM image, 0.41 mmol L^{-1}; (b) TEM image, 0.82 mmol L^{-1}; (c) DLS result, 0.41 mmol L^{-1}; (d) DLS result, 0.82 mmol L^{-1}; (e) and (f) mesostructures and section views of the equilibrium morphology of PD aggregates versus concentration φ_P. Beads W were not shown for the sake of brevity.

length and time unit, respectively. A DPD length unit is equal to the bead interaction range, and a time unit is the time taken for a bead to diffuse its own radius under thermal fluctuations. All simulations started with a randomly dispersed configuration, and the total simulation involved 50,000 steps, which was long enough for the system to reach equilibrium (Fig. S3). The spring constant was fixed at 4.0, which could foster reasonable results in these study systems.

4. Results and discussion

4.1. Concentration-dependent morphologic changes of blank PD aggregates

Because morphology has a significant impact on the micelle stability and capability of drug loading, the influence of concentration on the morphology of PD aggregates were investigated here (Dalhaimer et al., 2004; Geng et al., 2007; Sharma et al., 2010). The temperature was kept at 30 °C.

In aqueous solution, both the morphology and the size of PD aggregates were affected by the concentration of PD. As shown in Fig. 2, when PD concentration was at 0.41 mmol L^{-1}, spherical micelles with the average diameter nearly 50 nm were formed (Fig. 2a). At 0.82 mmol L^{-1}, vesicles combined with a small number of spherical micelles, and tubes were observed. Both the average diameter of vesicles and tubes were about 120 nm, much larger than that of micelles 20 nm. The micelles formed in the concentration of 0.82 mmol L^{-1} were much smaller than those that formed at 0.41 mmol L^{-1}. This may be because they form in the pre-equilibrium process from the fissions of vesicles and tubes (Fig. 2b). DLS indicated that, at 0.41 mmol L^{-1}, the size of spherical micelles exhibited narrow and monomodal distributions (PDI = 0.304) with an average diameter of 62.16 nm (Fig. 2c). There were two peaks for the diameter distribution of PD aggregates at 0.82 mmol L^{-1} (Fig. 2d). Peak 1 was observed at 29.06 nm, which was mainly attributable to the spherical micelles. Peak 2, which was observed at 135.58 nm, was mainly attributable to the vesicles. It should be noted that the DLS dimensions reported for anisotropic tube-like particles herein were actually sphere-equivalent diameters that did not provide accurate information regarding either tube length or tube width. Nevertheless, DLS observations of large particles and greater DPI (0.684) were useful indications of the presence of tube-like morphologies in the mixed phase. Even though the micelles shrank during the drying process and water evaporated under high vacuum during TEM imaging, the diameters of the PD aggregates obtained by DLS were hydromechanical. An increase in the micelle diameter obtained from DLS was reasonable (Giacomelli et al., 2006; Prabaharan et al., 2009). The results of these two methods were found to complement each other very well.

Fig. 2e and f shows the equilibrium morphology of PD aggregates versus concentration (volume fraction φ_P) at the mesoscopic scale obtained from DPD simulation. At low concentrations (φ_P = 0.02), small spherical micelles were formed with beads A and B in hydrophobic core and G in hydrophilic shell. As the concentration increased (φ_P = 0.10), vesicles appeared. G beads constituted the inner and outer hydrophilic layers, and beads A and B formed the hydrophobic shell. When the concentration of PD fell within the range of 0.10–0.18, the vesicles were stable and their

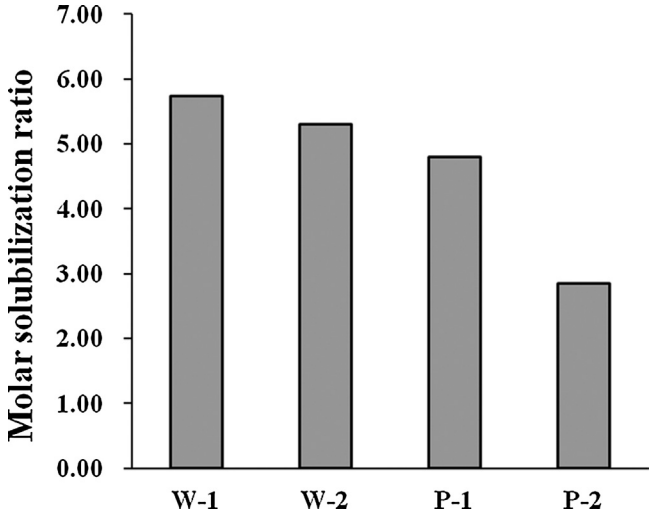

Fig. 3. MSR for different groups at 24 h (30 °C).

Please cite this article in press as: Ding, H., et al., Solubilization of menthol by platycodin D in aqueous solution: An integrated study of classical experiments and dissipative particle dynamics simulation. Int J Pharmaceut (2015), http://dx.doi.org/10.1016/j.ijpharm.2015.01.033

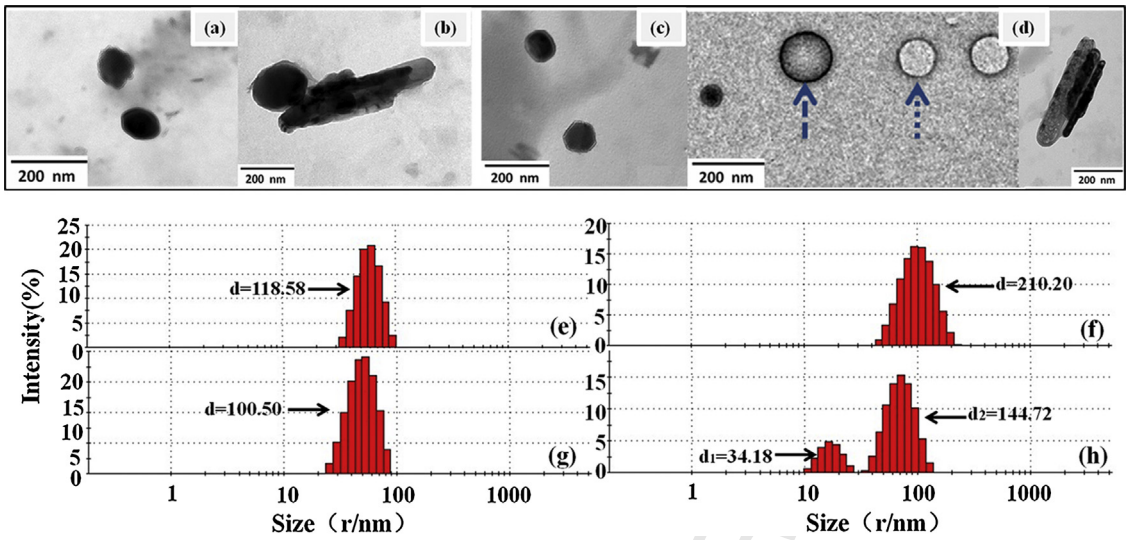

Fig. 4. Morphology of M-loaded PD aggregates.TEM images: (a) W-1, (b) W-2, (c) P-1, and (d) P-2. In P-2, the dashed line points to the M-loaded PD aggregates and the dotted line points to the blank PD vesicles. DLS results: (e) W-1, (f) W-2, (g) P-1, and (h) P-2.

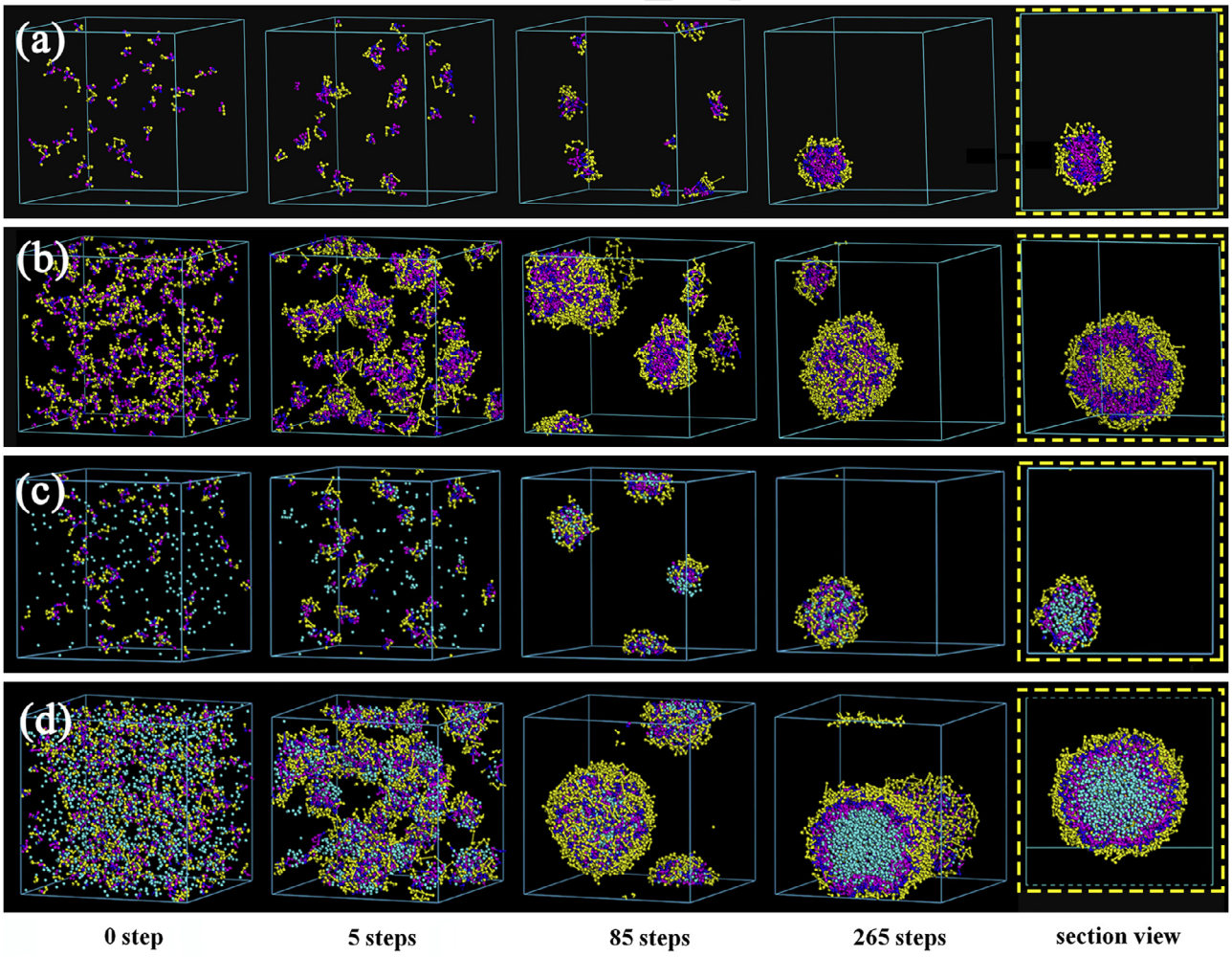

Fig. 5. Aggregating process of blank PD aggregates and solubilization process of M at method W: (a) blank PD-1, (b) blank PD-2, (c) W-1, and (d) W-2.

Please cite this article in press as: Ding, H., et al., Solubilization of menthol by platycodin D in aqueous solution: An integrated study of classical experiments and dissipative particle dynamics simulation. Int J Pharmaceut (2015), http://dx.doi.org/10.1016/j.ijpharm.2015.01.033

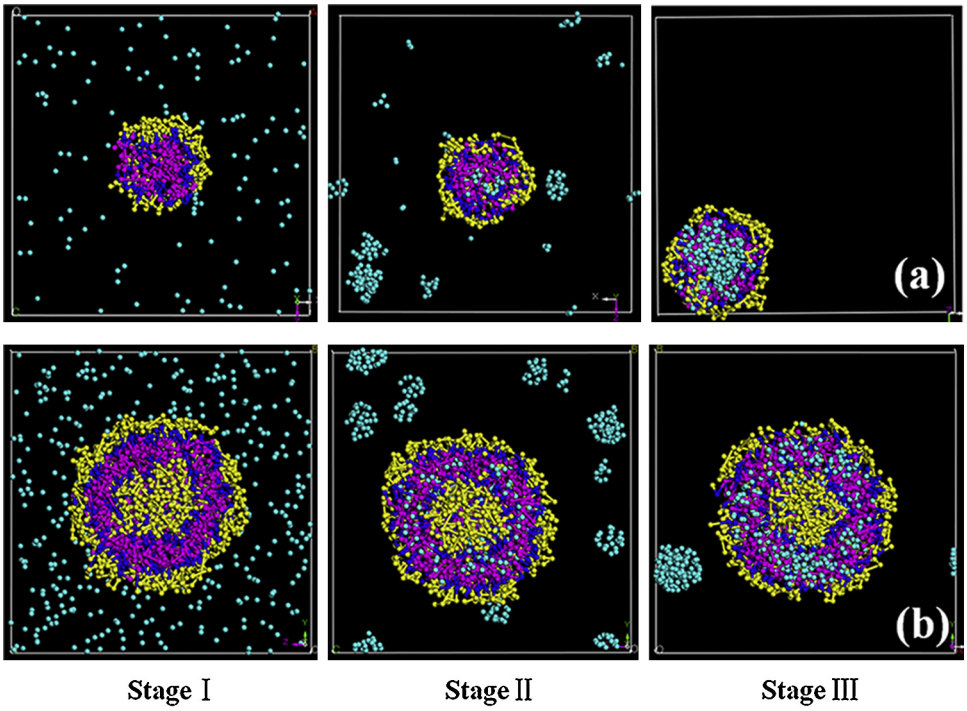

Fig. 6. Solubilization of M at different concentrations, method P, (a) P-1; (b) P-2.

size increased with increasing concentration. Tubes with cross sections similar to vesicles were observed at $\varphi_P = 0.19$. Though these DPD findings were not identical to the results from TEM, they showed the same trend.

4.2. PD concentration and solubility of M in aqueous solution

The amount of solubilizer plays a vital role in the solubilization process. The influence of PD's concentration on the solubilization of M was investigated, and two different methods of adding M to the sample were taken into consideration. One was dissolved the mixture powder of M and PD in water and shaken in a constant temperature bath to form mixed aggregates. The other was dissolved M in the aqueous solution of blank PD aggregates and shaken in a constant temperature bath to form mixed aggregates. The temperature was controlled at 30 °C. In the first case, M molecules were surrounded by PD molecules as if in wrapping, so this method is called "W". In the later case, M gradually entered the PD aggregates, we named this method as "P" for "permeation." Each method was carried out under two concentrations of PD, 0.41 mmol L^{-1} (marked "1") and 0.82 mmol L^{-1} (marked "2") in accordance with the laboratory experiment presented in Section 4.1. Group W-1 was subjected to the first method of addition at a PD concentration of 0.41 mmol L^{-1}; group W-2 was subjected to the first method of addition at a PD concentration of 0.82 mmol L^{-1}. P-1 and P-2 were given the corresponding treatments.

The capacity of solubilization can be quantified by the molar solubilization ratio (MSR), which is often calculated as follows (Edwards et al., 1991; Porter, 1994):

$$\mathrm{MSR} = \frac{S - S_{\mathrm{CMC}}}{C_S - \mathrm{CMC}} \quad (3)$$

here C_s is the concentration of PD, CMC is the critical micelle concentration of PD, S is the total apparent solubility of M, and S_{CMC} is the apparent solubility of M when the PD concentration is CMC. This is equal to the concentration of saturated aqueous solution of M.

In laboratory experiments, the apparent solubility of M can be obtained by gas chromatography. The PD aggregates can be destroyed by high injector temperature and the part of M molecules solubilized into PD aggregates can be released and detected. When the PD concentration is larger than its CMC, the solubility of M obtained by GC consist of two parts: the part solubilized into PD aggregates and the part in water aqueous, thus we name it the total apparent solubility S. In computer simulations, the number of M molecules solubilized into PD aggregates (N_1) and the number of PD molecules in aggregates (N_2) can be counted respectively by perl script, and the molar solubilization ratio can be calculated by $\mathrm{MSR} = N_1/N_2$.

The CMC of PD was determined to be 0.05 mmol L^{-1} by surface tension method (Supplementary data). When shaken for 24 h, the MSR for solutions W-1 and W-2 showed no significant differences (Fig. 3), but the amount of PD in the latter case was twice the

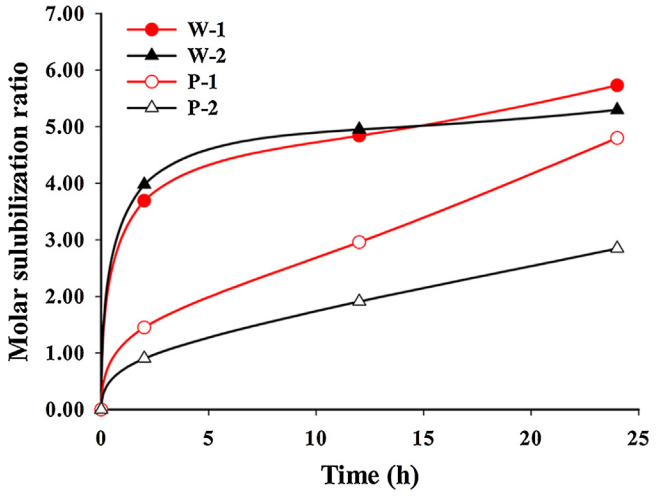

Fig. 7. MSR for different groups over time (30 °C).

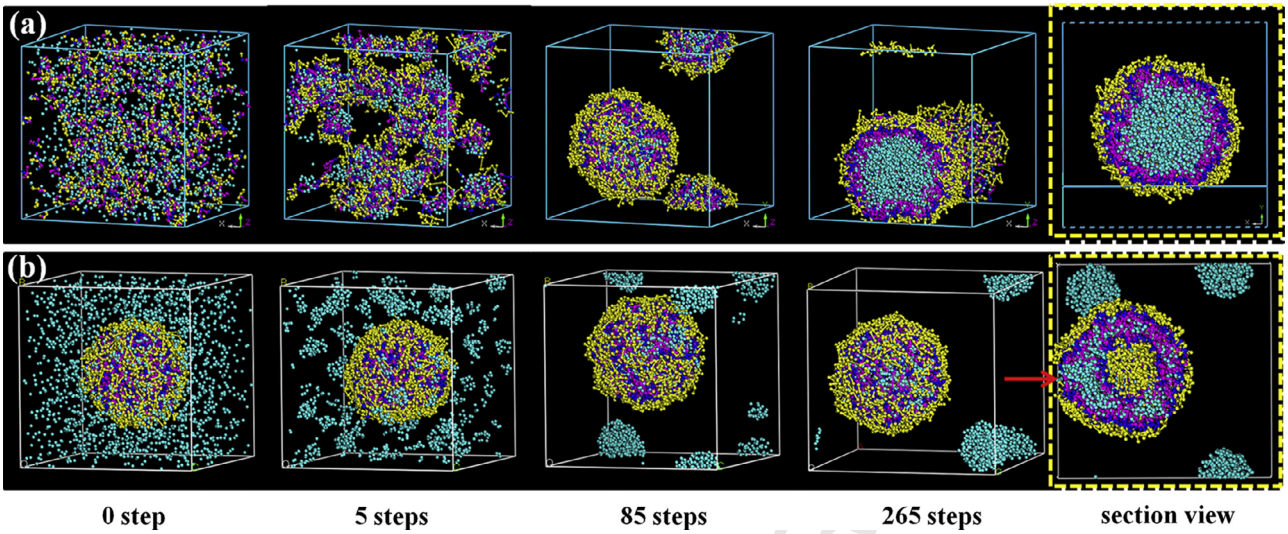

Fig. 8. Solubilization process and different methods of addition (a) W-2; (b) P-2.

former, and the mole of M solubilized into PD aggregates showed the same tendency. This was because W-1 and W-2 shared the similar initial state and solubilization process, which caused the aggregates to have almost the same morphology. The solubility of M only depended on the concentration of PD. The M-loaded PD aggregates for W-1 were spherical micelles with an average diameter of 118.58 nm (Fig. 4a and e). Aggregates in W-2 were mainly spherical micelles and a few tubes, the average diameter was 210.20 nm (Fig. 4b and f). The results of DPD (Fig. 5) can give reasonable explanation about this. It can be seen that, at higher concentrations, the small aggregates became easier to gather because of the increased rate of collision, thus promoting the formation of larger aggregates. In comparison, the aggregating process of blank PD aggregates are also given in Fig. 5a and b. Both the aggregating process and the final morphologies of M-loaded PD aggregates showed almost same as blank PD aggregates.

The MSR of P-2, 2.85, was much smaller than that of P-1, 4.80 (Fig. 3). This means that the mole of M solubilized by PD did not change considerably as the concentration of PD increases by this kind of adding method. After comparing the results of morphology experiments, we found that the increase in diameter of aggregates in P-2 was much less than that in P-1. In P-1, the initial morphology of blank PD aggregates was spherical micelles with an average diameter of 62.16 nm (Fig. 2c). After solubilization, the average diameter of these M-loaded spherical micelles increased to 100.50 nm (Fig. 4c and g). In P-2 there were two initial morphologies, the dominant one was the vesicle (d = 135.58), and the other was a spherical micelle (d = 29.06) (Fig. 2d). After solubilization, the diameter of these aggregates increased to 144.72 nm and 34.18 nm, respectively (Fig. 4d and h). This may be because of differences in the initial morphology of the blank PD aggregates.

In addition, the DPD simulation method was adopted to study the intrinsic mechanism at the molecular level. The results demonstrated the difference between the two solubilization processes. At the beginning, M dispersed in aqueous solution, then began to self-aggregate and integrate into PD aggregates. For spherical micelles, M was located at the hydrophobic cores. With more and more menthol molecules penetrated into micelles, PD molecules stretched and gradually became the outer protect layer wrapping around the M aggregates (Fig. 6a). For vesicles, M was located at the hydrophobic shells, which were sandwiched and hard-packed between the inner and outer hydrophilic layers. This configuration might discourage further diffusion of M molecules, thus limiting solubilization capacity (Fig. 6b).

As indicated by the findings listed above, when method W was used to add M, higher concentrations of PD were found to lead to greater solubility. While method P was used, the solubility of M did not change considerably as the concentration of PD increased. Different methods of adding M caused PD to show different solubilization capacities at the same concentration.

4.3. Method of adding M and solubilization efficiency in aqueous solution

Given the strong volatility of M, the less time spent in the solubilization process, the more M conserved. Herein, the influence of the method of addition of M on the solubilization rate was investigated. The samples in this part were still prepared at 30 °C and the amount solubilized as indicated by MSR was calculated after 24 h.

Fig. 7 shows the variation of MSR over time. During the first 2 h, the MSR of both W-1 and W-2 increased sharply and became significantly higher than that of P-1 and P-2. From 2 h to 12 h and 12 h to 24 h, the MSR of W-1 and W-2 increased slowly and that of P-1 and P-2 showed an almost linear uptrend. However, the MSR of W-1 and W-2 was still larger than that of P-1 and P-2 at 12 h and 24 h.

To determine molecular details associated with these two methods of adding M, DPD simulation was used to study the

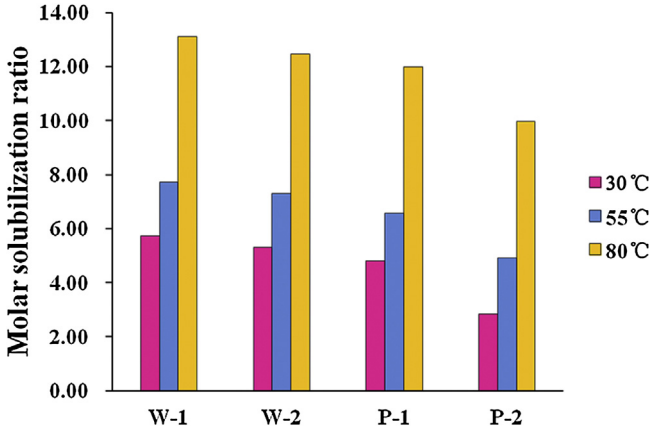

Fig. 9. MSR of different groups at different temperatures (24 h).

Please cite this article in press as: Ding, H., et al., Solubilization of menthol by platycodin D in aqueous solution: An integrated study of classical experiments and dissipative particle dynamics simulation. Int J Pharmaceut (2015), http://dx.doi.org/10.1016/j.ijpharm.2015.01.033

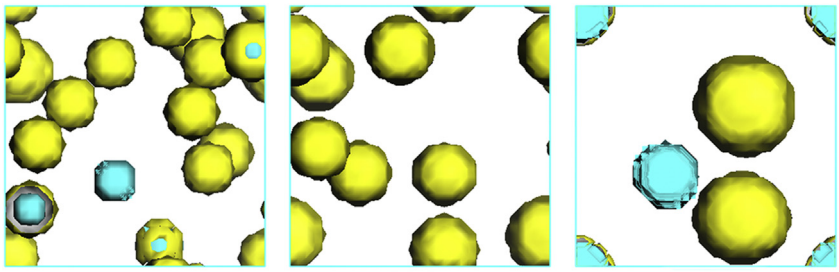

Fig. 10. MesoDyn morphology of M-loaded PD aggregates at different temperature.

dynamic solubilization process. As shown in Fig. 8a, in the W-2 case, M and PD dispersed uniformly in the aqueous solution at the initial state. Driving by the hydrophobic interaction, aggregates of different sizes were gradually formed by PD and M molecules. At 85 steps, almost all of M molecules were wrapped into different aggregates by PD molecules. During this period, the sizes of PD aggregates increased sharply, and M nearly saturated the PD aggregates. After that, the solubilization rate dropped. In the P-2 case, M entered the PD micelles. The space in the hydrophobic shell was gradually filled by M molecules, so the amount of M loaded by PD aggregates increased in an almost liner upward trend. However, at 265 steps, there was still small portion of M molecules in aqueous solution. That is because, during this solubilization process, M had to cross the hydrophilic sugar layer, which made the permeation more difficult and time-consuming. A breach was observed in the outer hydrophilic layer of M-loaded PD vesicle (Fig. 8b). This may indicate that the amount of M loaded had reached its limit. This was consistent with the laboratory results. It can be concluded that, at this temperature, the method of addition of M had a significant influence on the efficiency of M solubilization by PD in aqueous solution and that method W was beneficial to solubilization.

4.4. Temperature and solubility of M in aqueous solution

Temperature has a considerable influence on the efficiency of solubilization. In this study, three different temperatures (30 °C, 55 °C, and 80 °C) were studied to evaluate the effects of temperature on the solubilization of M (Table S5), the preparation time for all sample solutions was 24 h. As shown in Fig. 9, the MSR increased with temperature, and the effect was especially obvious at high temperatures 80 °C in all groups. These mean that high temperatures could improve the solubilization efficiency of M by PD. The value of MSR of these four systems at 55 °C and 80 °C shared the same trend with the one at 30 °C, and method W was more efficient at all temperatures examined. From the results of MesoDyn (Fig. 10), it can be seen that, M-loaded PD aggregates shared almost the same morphology at different temperature and their size enlarged with temperature rising.

5. Conclusion

In this study, we first investigated the morphology of PD aggregates in aqueous solution. PD preferred to form spherical micelles at a low concentration (0.41 mmol L^{-1}), but it tended to form vesicles at a high concentration (0.82 mmol L^{-1}). In the solubilization experiments, three factors were taken into consideration: concentration of PD, method of adding M and preparation temperature. The results showed that high concentrations of PD could lead to increases in solubility of M. The solubilization performance of PD was found to be closely associated with the method of addition of M. Method W showed obvious superiority. High temperatures were found to favor solubility of M, and the effect was especially obvious at high temperatures.

This study integrated a classical experiment and computer simulation to investigate the solubilization of a hydrophobic drug by saponin. This study not only provides comprehensive information on multiple scales but also a thorough understanding of the solubilization effect of saponins. It may be of great significance to the further development and application of natural solubilizers in the pharmaceutical industry.

Acknowledgments

This work was financially supported by the National Natural Science Foundation of China (81073058), Innovation Team Foundation of Beijing University of Chinese Medicine, Beijing (2011-CXTD-11, Research Center of TCM-information Engineering), Program for Excellent Talents in University (NCET-12-0803) and Excellent Talents Training Subsidy Scheme of Beijing (2013D009999000003). We would also like to thank Chemcloud Computing of Beijing University of Chemical Technology for their computational resources and assistance. We thank LetPub (www.letpub.com) for its linguistic assistance during the preparation of this manuscript.

Appendix A. Supplementary data

Supplementary data associated with this article can be found, in the online version, at http://dx.doi.org/10.1016/j.ijpharm.2015.01.033.

References

Buxton, G.A., Clarke, N., 2007. Drug diffusion from polymer core–shell nanoparticles. Soft Matter 3, 1513–1517.
Chengyuan, L., Weilin, L., Hanqing, Z., Bingru, R., 2003. The advance on the research of chemical constituents and pharmacological activities of *Mentha haplocalyx*. Chin. Wild Plant Resour. 9–12.
Dalhaimer, P., Engler, A.J., Parthasarathy, R., Discher, D.E., 2004. Targeted worm micelles. Biomacromolecules 5, 1714–1719.
Ding, H., Shi, X., Dai, X., Yin, Q., Qiao, Y., 2013. A mesoscopic simulation study on the solubilization of menthol by platycodin D. J. Eng. Sci. Technol. Rev. 6, 125–129.
Edwards, D.A., Luthy, R.G., Liu, Z., 1991. Solubilization of polycyclic aromatic hydrocarbons in micellar nonionic surfactant solutions. Environ. Sci. Technol. 25, 127–133.
Fraaije, J.G.E.M., van Vlimmeren, B.A.C., Maurits, N.M., Postma, M., Evers, O.A., Hoffman, C., Altevogt, P., Goldbeck-Wood, G., 1997. The dynamic mean-field density functional method and its application to the mesoscopic dynamics of quenched block copolymer melts. J. Chem. Phys. 106, 4260.
Geng, Y., Dalhaimer, P., Cai, S., Tsai, R., Tewari, M., Minko, T., Discher, D.E., 2007. Shape effects of filaments versus spherical particles in flow and drug delivery. Nat. Nanotechnol. 2, 249–255.
Giacomelli, C., Le Men, L., Borsali, R., Lai-Kee-Him, J., Brisson, A., Armes, S.P., Lewis, A. L., 2006. Phosphorylcholine-based pH-responsive diblock copolymer micelles

as drug delivery vehicles: light scattering, electron microscopy, and fluorescence experiments. Biomacromolecules 7, 817–828.
Groot, R.D., Warren, P.B., 1997. Dissipative particle dynamics: bridging the gap between atomistic and mesoscopic simulation. J. Chem. Phys. 4423–4435.
Groot, R.D., Madden, T.J., 1998. Dynamic simulation of diblock copolymer microphase separation. J. Chem. Phys. 108, 8713–8724.
Guo, X., Zhang, L., Qian, Y., Zhou, J., 2007a. Effect of composition on the formation of poly(DL-lactide) microspheres for drug delivery systems: mesoscale simulations. Chem. Eng. J. 131, 195–201.
Guo, L., Zhang, C., Li, L., Xiao, Y.Q., 2007b. Advances in studies on *Platycodon grandiflorum*. China J. Chin. Mater. Med. 32, 181–186.
Haiping, Z., Zhenggen, L., Genhua, Z., Jing, Z., Yun, L., Minxian, S., Ming, Y., 2012. Discussion on the holistic reevaluation of the commercial Yinqiao San serial traditional Chinese patent medicines. CJTCMP 2779–2781.
Hoogerbrugge, P.J., Koelman, J.M.V.A., 1992. Simulating microscopic hydrodynamic phenomena with dissipative particle dynamics. Europhys. Lett. 155–160.
Ingólfsson, H.I., Lopez, C.A., Uusitalo, J.J., Jong, D.H., Gopal, S.M., Periole, X., Marrink, S.J., 2013. The power of coarse graining in biomolecular simulations. WIREs: Comput Mol Sci.
Itoh, M., Koyama, K., Minowa, Y., Shirakawa, Y., 1986. Aqueous preparation containing vitamin E and saponins. Google Patents.
Jiangsu, N.M.C.O., 1986. Atlas of Traditional Chinese Medicines. Shanghai Science and Technology Press, Shanghai.
Kulperger, R.J., 1996. Enzymatic solutions containing saponins and stabilizers. Google Patents.
Mukherjee, S., Das, P., Sen, R., 2006. Towards commercial production of microbial surfactants. Trends Biotechnol. 24, 509–515.
Porter, M., 1994. Handbook of Surfactants. Chapman and Hall, UK.
Prabaharan, M., Grailer, J.J., Pilla, S., Steeber, D.A., Gong, S., 2009. Amphiphilic multi-arm-block copolymer conjugated with doxorubicin via pH-sensitive hydrazone bond for tumor-targeted drug delivery. Biomaterials 30, 5757–5766.
Ramos-Rodríguez, D., Rodriguez-Hidalgo, M., Soto-Figueroa, C., Vicente, L., 2010. Molecular and mesoscopic study of ionic liquids and their use as solvents of active agents released by polymeric vehicles. Mol. Phys. 108, 657–665.
Rodrigues, L., Banat, I.M., Teixeira, J., Oliveira, R., 2006. Biosurfactants: potential applications in medicine. J. Antimicrob. Chemoth. 57, 609–618.
Sasaki, Y., Mizutani, K., Kasai, R., Tanaka, O., 1988. Solubilizing properties of glycyrrhizin and its derivatives solubilization of saikosaponin-a, the saponin of bupleuri radix. Chem. Pharm. Bull. 36, 3491.
Sharma, G., Valenta, D.T., Altman, Y., Harvey, S., Xie, H., Mitragotri, S., Smith, J.W., 2010. Polymer particle shape independently influences binding and internalization by macrophages. J. Control Release 147, 408–412.
Soeder, C.J., Papaderos, A., Kleespies, M., Kneifel, H., Haegel, F., Webb, L., 1996. Influence of phytogenic surfactants (quillaya saponin and soya lecithin) on bio-elimination of phenanthrene and fluoranthene by three bacteria. Appl. Microbiol. Biot. 44, 654–659.
Sun, H., Chen, L., Wang, J., Wang, K., Zhou, J., 2011. Structure–function relationship of the saponins from the roots of *Platycodon grandiflorum* for hemolytic and adjuvant activity. Int. Immunopharmacol. 11, 2047–2056.
Urum, K., Pekdemir, T., 2004. Evaluation of biosurfactants for crude oil contaminated soil washing. Chemosphere 57, 1139–1150.
Walthelm, U., Dittrich, K., Gelbrich, G., Schöpke, T., 2001. Effects of saponins on the water solubility of different model compounds. Planta Med. 67, 49–54.
Yanjun, L., Jinming, Z., 2011. Discussion on the research thought and method of the meridian guiding theory of Platycodon root. Pharm. Clin. Chin. Mater. Med. 50–52.

Please cite this article in press as: Ding, H., et al., Solubilization of menthol by platycodin D in aqueous solution: An integrated study of classical experiments and dissipative particle dynamics simulation. Int J Pharmaceut (2015), http://dx.doi.org/10.1016/j.ijpharm.2015.01.033